

# STUDIES ON TRANSIENT-STAGE-SCALE GROWTH ON Fe-22wt.% Cr ALLOYS CONTAINING 120 PPM La + 270 PPM Ce

L. M. Fernandez Diaz<sup>1,3</sup>, J. Zhu<sup>1,3</sup>, G. R. Holcomb<sup>2</sup>, P. D. Jablonski<sup>2</sup>, D. E. Alman<sup>2</sup>, S. Sridhar<sup>1,3</sup>

<sup>1</sup>National Energy Technology Laboratory, 626 Cochran Mill Road, Pittsburgh, PA 15236, USA.

<sup>2</sup>National Energy Technology Laboratory, 1450 Queen Avenue SW, Albany, OR 97321, USA.

<sup>3</sup>Department of Materials Sciences and Engineering, Carnegie Mellon University, 5000 Forbes Ave, Pittsburgh, PA 15213, USA.

Keywords: reactive elements, high temperature oxidation, high chromium content iron alloys

## Abstract

Reactive elements (RE), such as Ce, La and Y, are known to improve oxidation resistance of Fe based alloys that form Cr<sub>2</sub>O<sub>3</sub> scales. The current investigation aims to characterize the oxide scale in a Fe-22 wt.% Cr alloy containing 120 ppm La and 270 ppm Ce (added during melt-stage processing) as a function of oxidation times (at 800°C in dry air) during the transient stage of scale formation. The surface oxidation processes were imaged in-situ through a Confocal Scanning Laser Microscope (CSLM). The results are correlated with post-experiment characterization through Field Emission Gun (FEG) - SEM and dual beam Focus Ion Beam (FIB) - SEM. The evolution of the reactive-elements-containing scale, its morphology and composition are determined.

## Introduction

The influence of reactive elements (RE) on lowering alloy-oxidation rates has been well established,<sup>1-4</sup> but even though several mechanisms have been suggested, no accordance has been reached.

Ecer and Meier studied the mechanism of Ni-Cr alloys containing 44 and 50 wt. % Cr.<sup>5</sup> The oxidation process is complex and it cannot be described by a single model. The growth of the Cr<sub>2</sub>O<sub>3</sub> oxide occurs by outwards Cr diffusion. Cr is transported to the scale, resulting in bulging, cracking and void incorporation. Giggins and Pettit studied the effect of ThO<sub>2</sub> dispersion in Ni-Cr alloys.<sup>1</sup> As Cr is removed from the metal to the oxide, the number of ThO<sub>2</sub> particles increase near the alloy/oxide interface. Eventually, ThO<sub>2</sub> particles impede transport of Cr atoms to the oxide. However, it is not known if the number of ThO<sub>2</sub> particles is enough to impede Cr diffusion.<sup>4</sup> Stringer et al.<sup>1</sup> proposed that dispersed CeO<sub>2</sub> and Y<sub>2</sub>O<sub>3</sub> in Ni-Cr alloys act as nucleation sites for Cr<sub>2</sub>O<sub>3</sub>. Ecer and Meier showed the effects of Ce additions on Ni-Cr alloys and the superficial application of CeO<sub>2</sub> powders on Ni-Cr and Fe-Cr alloys. RE oxides were suggested to act as nucleation sites. After the transient stage is over, cerium ions would segregate to the oxide grain boundaries and decrease the transport through them. Migration of the solute cloud with the grain boundary would involve a reduced level of atomic movement at the boundary. Thanneeru et al.<sup>6</sup> studied the high-temperature oxidation kinetics of steels in the presence of nanocrystalline ceria (NC) and La<sup>3+</sup> doped nanocrystalline ceria (LDN) coatings. Slower scale growth and finer grain structure with increased porosity were found as the La concentration was increased in LDN coatings.

In this paper Fe-22wt.%Cr alloy containing 120 ppm La + 270 ppm Ce were oxidized for 0, 5, 15, 30 and 60 minutes in air at 800°C. These conditions cover both the transient (0-30 min) and steady state (60 min) stages of scale development.<sup>7</sup>

## Experimental

An alloy (F<sub>2</sub>) with levels of 120 ppm La + 270 ppm Ce was prepared based on a nominal composition of Fe-22Cr-0.5Mn-0.1Ti (weight percent alloys). Glow Discharge Mass Spectroscopy (GDMS) was used to analyze rare earth element content of the alloy. The alloy chemistry is shown in table 1 below.

Sample chemistry.

El./Mat	B	F	Na	Mg	Al	Si	P	S	Cl	K	Ca	Ti	V	Cr
F <sub>2</sub> [wt%]	0.02	<0.01	0.04	0.2	330	8.3	16	46	0.12	<0.05	0.12	770	12	Matrix
El./Mat	Mn	Fe	Co	Cu	Zn	Y	Zr	Nb	Mo	La	Ce	Pr	Nd	C
F <sub>2</sub> [wt%]	0.56	Matrix	23	8.4	<5	<0.5	0.91	=<30	1.7	290	610	54	19	0.019

Table 1. Composition of F<sub>2</sub>.

Samples were polished using SiC paper number 320 and subsequently numbers 800 and 1200. Grinding was done using diamond paste suspensions of 6, 3 and 1  $\mu\text{m}$ .

The oxidation experiments were carried out in the gold-image hot-stage of a Confocal Scanning Laser Microscope (CSLM)<sup>8</sup>. The furnace chamber was evacuated and refilled with dry air, which was subsequently allowed to flow for 10 minutes. The flow rate was around 500 ml/s. The required heating time from room temperature (RT) to 800°C was 40s and the samples were maintained at this temperature for 0, 5, 15, 30 and 60 minutes after which they were cooled to RT. Zero minute oxidation corresponds to heat up – immediate cool down (0 hold time).

The samples were polished and marked with a Vickers hardness indenter. These fiducial marks were used to allow the recognition of specific areas that could be of interest. Once the marks were made, the position of RE inclusions was easily locatable on the surface. Its evolution was followed with CLSM and the same places were examined again after oxidation. The marked surface was characterized before and after the experiments by a Philips XL Field Emission scanning electron microscope (SEM). The accelerating voltage determining the energy and wavelength of electrons in the electron beam was 10 kV. The resolution in the secondary electron mode at 10 kV was 3.5 nm at a working distance of 10 mm.

Cross sections were obtained by milling a rectangular hole (ca. 7 x 3  $\mu\text{m}^2$ ) on the surface with a focused ion beam (FIB) in Nova 600 DualBeam system. To avoid charge effects the surface was previously covered with 7.0 nm of Pt. The region of interest to be cross sectioned (around 20  $\mu\text{m}$ ) was encapsulated with 1  $\mu\text{m}$  of Pt to avoid damage while milling. The surface was cross sectioned to a depth of 4-5  $\mu\text{m}$  using a 30 kv Ga<sup>+</sup> ion beam with a current of ca. 0.5 nA. Cross-sections were obtained and SEM images of selected features in the cross-sections were taken. The sample surface was examined by SEM and FIB was used to cross-section specific SEM pre-localized areas.

## Results and Discussion

The terminology used to explain the results is summarized in fig. 1. The “RE sites” or “RE containing sites” are the locations where RE were found before oxidation and became large particles on the surface after oxidation. “Far RE sites” are the surface areas not immediately surroundings the RE sites and includes both nodules and base metal oxide material. The “Near RE sites” includes the immediate locations surrounding the RE formed particles. “Oxide

nodules” are formed during oxidation and found in the surface afterwards. The “bulk” is the base metal oxide material behind the nodules.

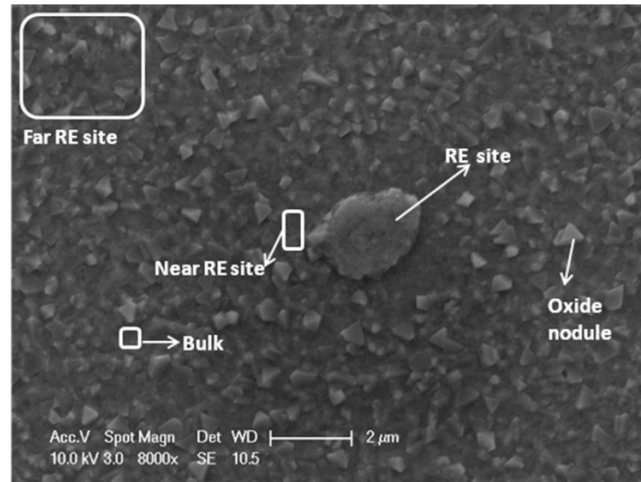


Figure 1. SEM microscopy showing the different parts analyzed in the surface of the sample.

Morphology

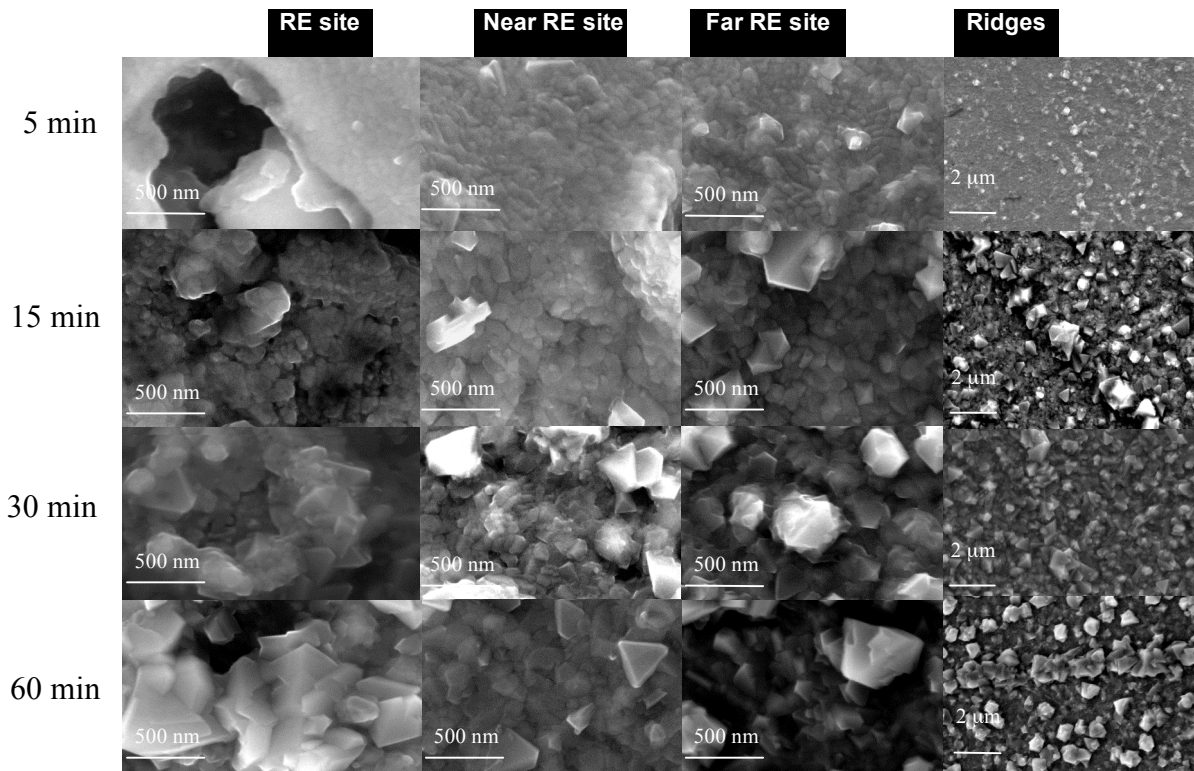


Figure 2. Secondary SEM images of F<sub>2</sub> samples oxidized for 5, 15, 30 and 60 min. The images show nucleation sites, areas around nucleation sites, areas far from the nucleation sites and ridges formed on the surface.

The oxidation of the samples was followed by CSLM. The surface starts oxidizing when the temperature reaches 600°C, corresponding to 40 s according to the temperature profile explained in the experimental section. The formation of ridges starts around 1:45 min oxidation. From this point on, only surface oxide growth is detected in the CSLM.

The samples used in the heating up – immediate cool down appeared a very intense copper color at the naked eye and their examination by SEM resulted in the obtaining of blurry images. Nevertheless, only few small nodules and no ridges are observable in the surface.

In figure 2 SEM pictures from different points of the surface: on particles, area surrounding particles, area far from particles and ridges; at different oxidation times: 5, 15, 30 and 60 minutes are shown.

The pictures show that the oxide nodule size is larger far from the RE-particles than in their vicinity, when comparing columns 2 and 3 in figure 2.

However, the size of the oxides formed on the particles appears to be largest (column 1 in fig. 2).

With time, the increase of oxide particles size on the RE containing sites is evident. As well, an increase of the oxide particle size is observable with time in the area surrounding these sites.

The size of the oxide particles far from the nucleation sites increase from 5 to 30 minutes. After 60 minutes the grain size seems comparable to the size after 30 minutes.

Regarding ridges, after 5 minutes oxidation they are small and barely distinguishable. After 15 minutes of oxidation they are very visible. The size of the nodules constituting the ridges size seem to be comparable at 15, 30 and 60 minutes.

## Composition

Summary of the composition in the main structural features of the surface.

Ridges						Base metal oxide					
El.(wt%)/t(min)	0	5	15	30	60	El.(wt%)/t(min)	0	5	15	30	60
<b>O K</b>	0	16.7	32	33	33.9	<b>O K</b>	2.6	6.6	16.7	15.5	17.7
<b>Cr K</b>	0	32.7	48.9	38.8	50.1	<b>Cr K</b>	22.8	25.2	23.5	32.5	35.2
<b>Mn K</b>	0	7.2	11.1	2.7	14.6	<b>Mn K</b>	0	1.2	0.5	3.1	2.1
<b>Fe K</b>	0	41.6	1.8	22.2	0	<b>Fe K</b>	74.6	67.1	56.7	48.7	44.4
<b>Ti K</b>	0	1.7	2.2	3.2	1.4	<b>Ti K</b>	0	0	0.2	0	0
Oxides Nodule						RE sites					
El.(wt%)/t(min)	0	5	15	30	60	El.(wt%)/t(min)	0	5	15	30	60
<b>O K</b>	0	12	19.4	24.1	25.1	<b>O K</b>	13.2	19.1	26.2	27	31.7
<b>Cr K</b>	0	30.9	40	30.9	42	<b>Cr K</b>	14.4	17.7	21.6	18.2	40.2
<b>Mn K</b>	0	3.3	4	8.9	12.4	<b>Mn K</b>	0	0.4	2.1	2.9	10.3
<b>Fe K</b>	0	53.8	44.2	35	20.3	<b>Fe K</b>	40.5	24	15.4	14.1	11.3
<b>Ti K</b>	0	0	0.2	0	0	<b>Ti K</b>	3.6	1	0.4	0.4	0.6
						<b>La L</b>	10.4	14	9.6	17.6	1.1
						<b>Ce L</b>	11.9	18.8	17.9	16.5	2.7

Table 2. Elemental composition after different oxidation times in different parts of the surface.

The compositional evolution of the reactive elements containing sites (table 2) with the oxidation time is summarized as follows: in general it can be said that the concentration of reactive elements (Ce, La, Ti) decrease with time at these sites while O, Cr, and Mn increase. La could have a tendency to diffuse towards the surface but only when the oxidation time is long enough, Cr and Mn oxides will cover it. This indicates the formation of chromium and manganese oxides over the reactive elements, forming a layer covering and burying them, which supports the hypothesis of RE acting as nucleation sites for chromium and manganese oxides.

The comparison of composition evolution with time between areas surrounding RE containing sites and areas far from them show that Ti amount is very little in the surface and its behavior is the same in both areas, far and near RE sites. The manganese concentration is much higher in case of sites far from the surface and it increases with oxidation time. Around RE sites the amount of Mn tends to decrease with time. Depleted Mn zones are also shown to be Cr depleted at 5 and 15 minutes of oxidation, while after this oxidation time the quantities of Cr are comparable at both far and near RE sites (being slightly higher near them). This phenomenon can also be justified by assuming the RE are acting as nucleation sites for Cr and Mn oxides. At short oxidation times REs are attracting Cr to become wrapped with Cr oxides. Longer oxidation times allow Cr to diffuse from the alloy towards RE sites and the Cr depleted area is no longer

observed. The explanation is not valid for Mn due to its much lower concentration in the bulk material. Regarding Fe, RE surrounding areas are rich in this element at low oxidation times (5 and 15 minutes; due to the lack of Cr and Mn). At 30 minutes its value drastically decreases in these zones, because of the higher amount of Cr. After 60 minutes oxidation the concentration of iron far and near the RE sites is comparable.

Regarding the base metal oxide composition (table 2) evolution with oxidation time, it can be said this oxide evolves to a mixture of Fe, Cr and Mn oxides (spinel) which enriches with time in Cr and Mn oxides, diminishing the fraction of Fe. Cr and Mn diffuse towards the surface with increasing oxidation time. The increase/decrease of the element concentrations diminishes in magnitude after 30 minutes indicating that steady state is reached. This time frame is in good agreement with the literature values for the conclusion of steady-state oxidation in similar alloys.<sup>9</sup> The composition near the particles is comparable to the bulk composition at all times, indicating that the presence of RE prevents the formation of chromium oxide nodules. This agrees with the results shown in the previous section, where it can be seen the zones near the particles are morphologically comparable to the bulk material.

The study of evolution of nodules composition (table 2) with oxidation time shows that the first nodules can be observed after 5 minutes oxidation. These initial oxide nodules are very rich in Fe. With oxidation time the composition evolves to oxides richer in Cr and Mn and poorer in Fe. Ridges are also found to be formed in the surface after 5 minutes of oxidation. They are made out mainly of Fe, Cr, O, Mn and some Ti (table 2). A parallel behavior between Cr and Mn can be observed. The oxygen concentration reaches steady state after 15 minutes and the amount of Ti does not vary much from that time.

The evolution with oxidation time of Fe, Cr, O, Mn and Ti contents on different parts of the surface can be summarized as follows:

- Fe: bulk > nodules > ridges (irregular behavior) ~ particle. Decreases with time, in all cases.
- Cr: ridges > nodules > bulk > particle (analogous behavior in ridges and nodules). Increases with time, in all cases.
- Mn: ridges > nodules > particle > bulk (but for 30 minutes, dramatic decrease in the ridges, keeps tendency in the nodules). Tendency to increase in all cases.
- Ti: ridges > particle > bulk = nodules. Increases with time in the ridges but decreases in the particles. Not significant in the bulk or in the nodules.

### Dual Beam FIB Cross-Sections

Figure 3 shows the cross sections obtained for the different oxidation times: before and after 0, 5, 15, 30 and 60 minutes and table 3 summarizes the sizes of the features found in the cross sections of the scale.

The cross section of an RE inclusion before oxidation showed a void which does not have any surrounding layer.

The cross sectioned particle in the sample corresponding to the 0-holding zone shows no observable oxide layer after this quick heating. Two phases seem to be differentiated in the RE particle. The particle in this case appears to be porous.

The images obtained after 5 minutes oxidation show no observable ridges on top of grain boundaries and no observable surface oxide scale.

After 15 minutes oxidation, the layer thickness is quite inhomogeneous and nodules are often found. There are other areas where the scale thins and it appears the bulk is forming a nodule surrounded by the oxides layer. Also a small amount of internal oxidation could be observed.

Preliminary TEM studies were carried out in a comparable RE dual phase particle of F<sub>2</sub> samples oxidized for 15 minutes. According to the EDX results on the TEM sample, Ti segregated in the upper part of the particle, closer to the scale, and the REs segregated to the lower part of the particle. If this is the case for the particle observed on the cross-section obtained with FIB, and

since Ti can segregate with RE elements, the lighter gray part is likely to be Ti-containing phase. Further EDS work is needed to confirm this postulation.

According to these initial results a division of the different phases in the particle can be made as shown in figure 3: region I (upper phase) is comprised of Ti oxides; region II (lower phase), would be comprised of RE oxides and region III would be a thin layer of chromium oxides.

A dual phase RE particle is also detected after 30 minutes oxidation. The average of scale thickness, 66 nm, was comparable to the thickness found after 15 minutes oxidation. As in the 15 minutes case, nodules were found. Also thinner sections in which the scale seemed to be surrounding a nodule formed by the bulk alloy were observed. Scale ridges were found to be about the same height as the ones formed after 15 minutes oxidation, but broader. After this oxidation time, a lighter layer underneath some sections of the scale could be observed.

After 60 minutes oxidation, the RE particle shows again two phases, but the lighter phase is dominant. The scale was found to be thicker than for 15 and 30 minutes oxidation. Nodules were also found in the scale, with a size comparable with the other oxidation times. In this sample voids were seen in the thicker parts of the scale. The opposite nodules, with a lighter core and where the scale is thicker, are from a material which is shown to be from a lighter color than the bulk. This lighter layer can be also found in some regions underneath the scale. Regarding ridges, they were found again on top of grain boundaries. The ridges are in this case a bit higher but broader.

Size of morphological features found in the cross-sectioned sample surfaces.

<i>Feature</i>	<i>Dimension</i>	Before oxidation	0 min	5 min	15 min	30 min	60 min
<i>RE sites</i>	Height, $\mu\text{m}$	1.1	0.72	1.14	1.74	1.74	1.87
	Width, $\mu\text{m}$	0.44	2.00	1.18	0.63	1.26	1.62
<i>Scale</i>	Thickness, nm				68.97	65.99	108.89
<i>Nodules</i>	Height, $\mu\text{m}$				0.17	0.20	0.19
<i>Ridges</i>	Height, $\mu\text{m}$				302.21	358.29	425.97
	Width, $\mu\text{m}$				616.48	660.54	1013.78

Table 3. Size of RE inclusion, nodules and ridges found in the cross-sectioned surfaces.

In figure 4 the evolution in width and height of measured ridges with oxidation time is shown. The width of ridges is greater than their height and they tend to increase in width rather than height during oxidation. Ridge height slightly increases from 15 to 30 minutes and then it remains constant. Ridges grow on top of grain boundaries<sup>10</sup> (figure 3) presumably because of preferential diffusion of Mn and Cr. Assuming that formation of grain boundaries in the scale will take place over the alloy grain boundaries, the increase in ridge width rather than ridge height could be indicative of RE blocking preferentially grain boundaries in the scale, but this explanation should be taken carefully, as this phenomenon is sometimes explained as a result of slower diffusion rate caused by thicker scale at the ridge<sup>11</sup>. As Cr and Mn are provided from the alloy their oxides are accommodated by lateral ridge growth.

Figure 5 shows a schematic representation of the phenomena occurring at the surface of these alloys during oxidation. Initially, only RE-containing inclusions are found at the surface. At the onset of oxidation RE particles migrate towards the surface and grain boundaries. Mn and Cr diffuse towards the surface where a scale rich in spinel starts to form. This spinel becomes richer in Cr and Mn and Cr oxides nodules grow over it. Cr and Mn diffuse preferentially along grain boundaries forming ridges on top of them. RE inclusions act as nucleation sites for Cr and Mn oxides, and the layer formed near them increases in thickness with time. Cr oxides nodules do not form in these areas as all the Cr forms the scale around RE. Analysis of the ridges inter-phase

morphology could suggest grain boundaries in the scale are blocked by REs. Size of the ion has been indicated to be the major factor in determining the extent of grain boundary adsorption of impurities in oxides<sup>3</sup>.  $Ti^{4+}$  size ( $r^{Ti^{4+}}=0.68\text{\AA}$ ,  $r^{Ce^{4+}}=1.01\text{\AA}$ ,  $r^{La^{3+}}=1.87\text{\AA}$ ) would explain its diffusion through the alloy grain boundaries, even if Ti behavior could be compared to RE.

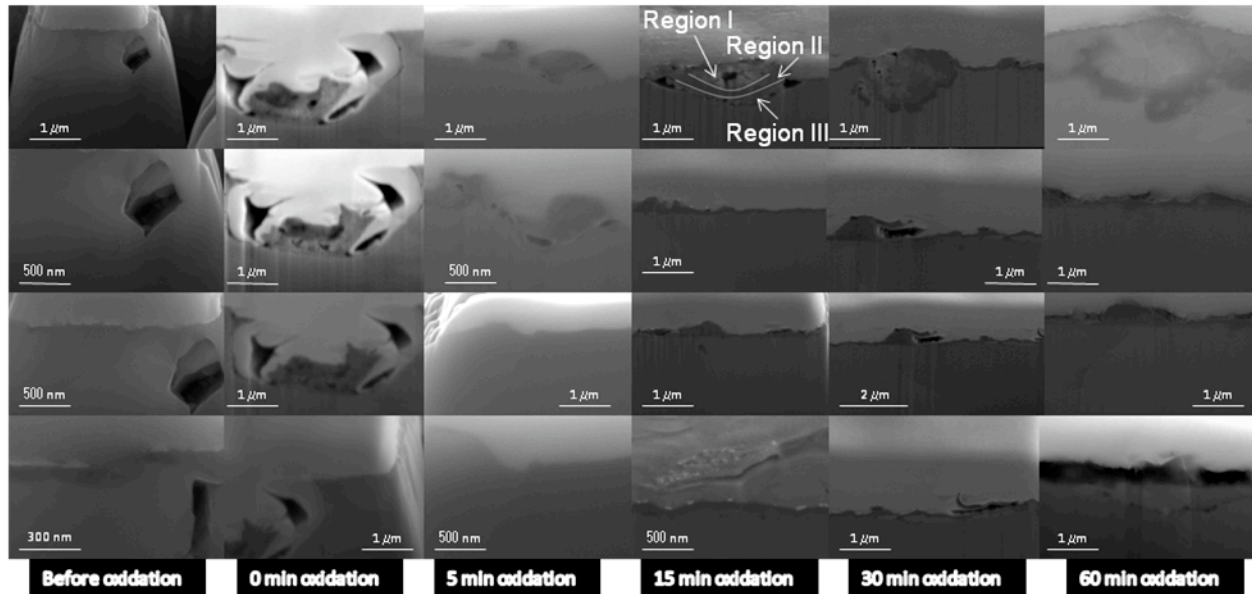


Figure 3. Cross sections before and after 0, 5, 15, 30 and 60 min. oxidation. Secondary images.

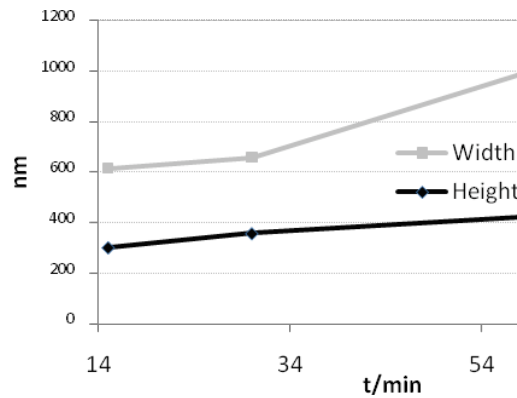


Figure 4. Evolution with time of the width and height of the ridges in the cross-sectioned areas.

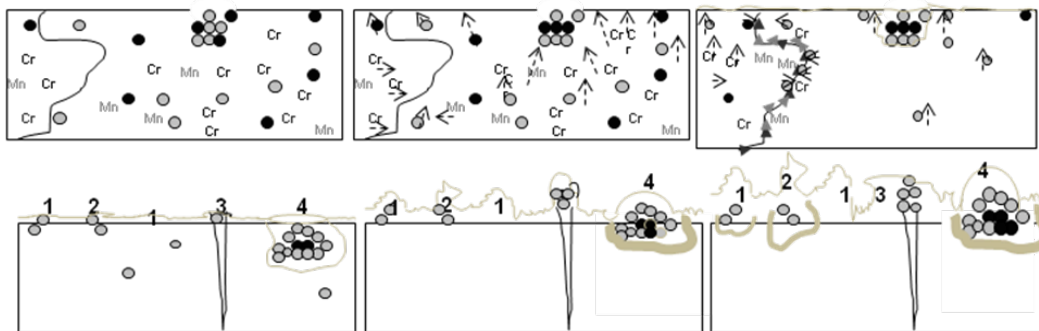


Figure 5. Schematic representation of evolution of scale with increasing oxidation time. **1 and 2:** particles formed on the surface (rich mainly in chromium oxides). Some of them contain Mn oxides. **3:** ridges of Cr and Mn oxides formed on the alloy grain boundaries. **4:** Potential RE nucleation sites. Cr and Mn oxides grow in these sites. ○ - RE particles, ● - Ti particles.

## Conclusion

The oxidation starts around the temperature of 600°C. The formation of ridges takes place around 65 s after oxidation begins. According to CLSM no superficial phenomena are visible from the formation of ridges. Formation of ridges or opening of holes in the surface can be observed within the first 90 s. From this point onward no relevant changes to the surface are observed. The morphology of the scale at 5 min is difficult to distinguish but after 15 minutes ridges and oxide particles in all points of the surface can be seen.

SEM results show an increase in the oxide particle size on the nucleation site, near the nucleation site and far from it with time. Ce and La are localized at specific sites in the surface (inclusions) and no significant amount can be found forming ridges, nodules or base metal oxide. RE act as nucleation sites for Cr and Mn oxides. They tend to be surrounded and buried by these oxides with increasing oxidation time. Cr depleted zones around RE are found at short oxidation times (5 and 15 minutes). These areas are also depleted of Mn. Areas around RE sites are comparable to bulk material, both morphologically and compositionally. Cr and Mn diffuse towards the surface with time. Transient stage of oxidation seems to be over at 30 minutes.

Base metal oxide material evolves with time, transforming spinel into oxides richer in Cr and Mn and poorer in Fe. Similar behavior is observed for oxide nodules and ridges. Ti is mainly present at RE sites and ridges. The Fe concentration is highest in the base metal oxide material, while Cr, Mn and Ti are more concentrated in ridges.

Features such as surface scale, nodules, and ridges are observable in the cross-sections only after 15 minutes oxidation.

The thickness of the scale is comparable in samples oxidized for 15 and 30 minutes, but increases for 60 minutes oxidation.

The RE particles appear to develop into dual phase particles with oxidation time. Two different nodules are found in the scale. Darker nodules appear to be simply the oxide formed the base metal while lighter nodules resemble a phase found in the RE particles. Further investigation into the composition of these nodules is planned.

Ridges are found in all cases above alloy grain boundaries. With increasing oxidation time they tend to broaden but do not significant increase in height.

Lighter layers can be found in some regions beneath the scale. These could be a possible relation to the lighter phase found in the RE particles.

## Acknowledgments

This technical effort was performed in support of the National Energy Technology Laboratory's on-going research in the study of the effects of rare earth elements on the high temperature oxidation of stainless steels under the RDS contract DE-AC26-04NT41817.

---

<sup>1</sup> J. Stringer, B. A. Wilcox and R. I. Jaffee: *Oxid. Met.* Vol. 11(1972), p. 5.

<sup>2</sup> G. M. Ecer and G. H. Meier: *Oxid. Met.* Vol. 13 (1979), p. 159.

<sup>3</sup> M. Ecer, Singh and G. H. Meier: *Oxid. Met.* Vol.18 (1982), p. 55.

<sup>4</sup> C. S. Giggins and F. S. Pettit: *Met. Trans.* Vol. 2 (1971), p. 1071.

<sup>5</sup> G. M. Ecer and G. H. Meier: *Oxid. Met.* Vol. 13 (1979), p. 119.

<sup>6</sup> R. Thanneeru, S. Pati., S. Deshpande and S. Seal: *Act. Mat.* Vol. 55 (2007), p. 3457.

<sup>7</sup> M. Hajduga and J. Kučera: *Oxid. Met.* Vol. 29 (1988), p. 121.

<sup>8</sup> H. Yin, H. Shibata, T. Emi and M. Suzuki: *ISIJ Int.* Vol. 37 (1997), p. 936.

<sup>9</sup> M. Hajduga and J. Kucera: *Oxid. Met.* Vol. 29 (1988), p. 121.

<sup>10</sup> L. M. Fernandez Diaz, J. Zhu, G. R. Holcomb, P. D. Jablonski, D. E. Alman, S. Sridhar, *Defects and Diffusion Forum*, in print (2008).

<sup>11</sup> Lars Mikkelsen, PhD thesis, Riso National Lab, Denmark (2003).